Spatial patterns of ecosystem carbon residence time and NPP-driven carbon uptake in the conterminous United States

Tao Zhou[1,2] and Yiqi Luo[2]

Received 25 January 2007; revised 9 June 2008; accepted 23 June 2008; published 27 September 2008.

[1] Ecosystem carbon (C) uptake is determined largely by C residence times and increases in net primary production (NPP). Therefore, evaluation of C uptake at a regional scale requires knowledge on spatial patterns of both residence times and NPP increases. In this study, we first applied an inverse modeling method to estimate spatial patterns of C residence times in the conterminous United States. Then we combined the spatial patterns of estimated residence times with a NPP change trend to assess the spatial patterns of regional C uptake in the United States. The inverse analysis was done by using the genetic algorithm and was based on 12 observed data sets of C pools and fluxes. Residence times were estimated by minimizing the total deviation between modeled and observed values. Our results showed that the estimated C residence times were highly heterogeneous over the conterminous United States, with most of the regions having values between 15 and 65 years; and the averaged C residence time was 46 years. The estimated C uptake for the whole conterminous United States was 0.15 P g C a^{-1}. Large portions of the taken C were stored in soil for grassland and cropland (47–70%) but in plant pools for forests and woodlands (73–82%). The proportion of C uptake in soil was found to be determined primarily by C residence times and be independent of the magnitude of NPP increase. Therefore, accurate estimation of spatial patterns of C residence times is crucial for the evaluation of terrestrial ecosystem C uptake.

Citation: Zhou, T., and Y. Luo (2008), Spatial patterns of ecosystem carbon residence time and NPP-driven carbon uptake in the conterminous United States, *Global Biogeochem. Cycles*, *22*, GB3032, doi:10.1029/2007GB002939.

1. Introduction

[2] Rising atmospheric CO_2 concentration, due to fossil fuel combustion and deforestation, has resulted in global warming [*Houghton et al.*, 2001]. To prevent dangerous anthropogenic interference with the climate system and to predict future environmental change, we have to quantify the magnitude and spatial distribution of carbon (C) uptake in terrestrial ecosystems. Recent analyses of the global C cycle indicate that terrestrial ecosystems absorb a significant proportion of anthropogenic CO_2 [*Schimel et al.*, 2001; *Canadell et al.*, 2007]. However, C uptake rates and their spatial distributions have not been well quantified [*Houghton*, 2003].

[3] Carbon uptake is regulated by C influx via photosynthesis and residence times in various plant and soil pools. The C cycle in an ecosystem usually initiates when plants fix CO_2 via photosynthesis. A portion of photosynthate is used to grow plant tissues while the rest is released back into the atmosphere via plant respiration. The plant tissues can live for several months (e.g., leaves and fine root) up to hundreds of years for wood in forests (i.e., longevity of plant tissues or residence times of carbon in plant pools). Dead plant materials (i.e., litter) are partially decomposed by microbes and partially incorporated into soil organic matter (SOM), which can store C in soil for hundreds and thousands of years (i.e., residence times of carbon in soil pools) before it is broken down to CO_2 through microbial respiration. Among the processes, carbon influx drives carbon cycling. The fraction of influx carbon that can be uptaken by an ecosystem is determined by residence times: the length of time a carbon atom can stay in plant and soil pools from the entrance via photosynthesis to the release back to the atmosphere via plant and microbial respiration (see *Luo et al.* [2001, 2003] for more discussion).

[4] Without changes in external driving forces such as disturbances and climate change, the C influx and efflux are gradually equilibrating so that the magnitude of C uptake approaches zero. However, the external driving forces, including climate change [*Dai and Fung*, 1993], CO_2 fertilization [*Cramer et al.*, 2001], increased N deposition [*Holland et al.*, 1997], and land use change [*Houghton et al.*, 1999] break up the balance of the ecosystem C cycle, and possibly cause more C influx to the ecosystem through net primary production (NPP) increase [*Nemani et al.*, 2003]. As a result, the NPP increase makes ecosystem C uptake possible in the next few decades despite the fact that global warming is likely to stimulate decomposition of

[1]State Key Laboratory of Earth Surface Processes and Resource Ecology, Beijing Normal University, Beijing, China.
[2]Department of Botany and Microbiology, University of Oklahoma, Norman, Oklahoma, USA.

0886-6236/08/2007GB002939$12.00

organic matter [*Cox et al.*, 2000]. It is fortunate that the spatial patterns of NPP changes are relatively well quantified by using ecosystem production models in concert with remote sensing techniques [*Field et al.*, 1995]. Those studies indicate that an apparent NPP increase trend exists in the conterminous United States [*Hicke et al.*, 2002]. Therefore, advances in spatial patterns of carbon residence times are crucial for modeling C uptake. Unfortunately, the spatial patterns of carbon residence times, to the best of our knowledge, have not been quantified for the conterminous United States.

[5] Several methods have been used to estimate the carbon residence times. One is an experimental approach that usually measures a certain standing stock of C pools and the corresponding fluxes; and then uses the ratio of stock divided by flux as the approximation of residence times [e.g., *Vogt et al.*, 1996]. This method is simple and easy to conduct, but the challenge is that not all standing stocks and fluxes of subpools can be easily measured (e.g., root mortality). Another method to estimate carbon residence times is to use C isotopes. Nuclear bomb tests in the 1960s caused a drastic increase of ^{14}C in the atmosphere. This so-called ''bomb carbon'' has been successively transferred from the atmosphere to plants and to soil organic carbon (SOC). Thus, the bomb carbon has been used as a tracer to estimate carbon residence times in various pools [e.g., *Gaudinski et al.*, 2001]. However, the residence times estimated from ''bomb carbon'' method for individual plant and soil pools have to be incorporated into models to estimate the ecosystem carbon residence times on regional scales.

[6] Other than those experiment-based methods, inverse analysis, which has recently become one major tool for data-model fusion [*Raupach et al.*, 2005], has been used to estimate carbon residence times [*Barrett*, 2002; *Luo et al.*, 2003; *Xu et al.*, 2006]. For example, inverse analysis was applied to estimate carbon residence times from six data sets obtained at the Duke Forest Free-Air CO_2 Enrichment (FACE) experimental site [*Luo et al.*, 2003; *White et al.*, 2005; *Xu et al.*, 2006]. The estimated carbon residence times, together with canopy photosynthesis, were used to characterize C uptake in that forest ecosystem [*Luo et al.*, 2003; *Xu et al.*, 2006]. *Barrett* [2002] applied inverse analysis technique to the Vegetation-And-Soil-Carbon-Transfer (VAST) model to estimate carbon residence times on the continental scale in Australia.

[7] The objective of this study is to evaluate the spatial patterns of C uptake in the conterminous United States under the current driving force of NPP increases. To achieve this goal, we focused our studies on three interrelated subobjectives. First, we used an inversion method to estimate the spatial patterns of carbon residence times. Second, we applied the NPP increase trend that has been monitored by remote sensing data [*Hicke et al.*, 2002] to evaluate C uptake. To evaluate relative importance of carbon residence times and strength of NPP increase on C uptake, we made two kinds of simulations. One assumed a spatially uniform NPP increase (i.e., each spatial grid has the same strength) as the driving force for the conterminous United States to evaluate the spatial patterns of C uptake caused mainly by the spatial patterns of carbon residence times. Two applied the actual spatial patterns of NPP increases [*Hicke et al.*, 2002] to evaluate the spatial patterns of C uptake caused by spatial patterns of both carbon residence times and NPP increases. Third, we conducted sensitivity analyses to evaluate impacts of observation errors, equilibrium assumption, and initial soil organic carbon on parameter estimation and on the C uptake.

[8] Note that this study focused on carbon uptake driven by NPP changes in various ecosystems with different residence times, which were estimated with an inversion method described below. Other mechanisms, such as fire and land use change, also influence land carbon sink/source by altering not only NPP but also residence times and pool sizes to cause disequilibrium of C cycling processes. Thus, carbon sink/source associated with the disequilibrium was not be fully accounted for in this study.

2. Methods and Materials

[9] The inverse analysis conducted in this study was based on a Terrestrial Ecosystem Regional (TECO-R) model, where 12 data sets were used for parameter estimation. The TECO-R model was developed by combining the Carnegie-Ames-Stanford-Approach (CASA) model [*Potter et al.*, 1993; *Field et al.*, 1995] with the Vegetation-And-Soil-Carbon-Transfer (VAST) model [*Barrett*, 2002] to estimate the spatial patterns of carbon residence times in the conterminous United States. The TECO-R model uses the CASA algorithms on net primary productivity (NPP), which was estimated from satellite observation and ground measurements, and the VAST algorithms for the relationships of C transfer among pools. The TECO-R model is described in Appendix A, with a schematic diagram shown in Figure 1 and the parameter definitions given in Table 1. The parameters estimated in this study included the maximum potential light-use efficiency (ε^*), C allocation coefficients among pools, and C residence times in individual plant and soil pools. The allocation coefficients and residence times of C in the individual pools were integrated to estimate the whole ecosystem residence times over the conterminous United States. To facilitate parameter estimation, this study divided soil organic carbon (SOC) and root biomass into three soil layers (top: 0–20 cm, middle: 20–50 cm, and bottom: 50–100 cm) as by *Barrett* [2002], instead of compartmentalized SOC according to decomposition rates as in the Century model [*Parton et al.*, 1987]. In this way, the state variables of root biomass and SOC in the model have a one-to-one correspondence with the respective observations and do not need extra mapping functions (or observational operators) as by *Luo et al.* [2003].

2.1. Data

[10] In this study, 12 observed data sets were used for the parameters estimation, which included three NPP data sets (i.e., NPP in leaves, stems, and roots), five biomass data sets (i.e., one for biomass of leaves, one for stems, and three for roots in three soil layers), one litter data set (i.e., fine litter mass), and three SOC data sets in the three soil layers. There were a total of 7660 observed data points, which contained 7 data points in fine litter, 468 data points in NPP, 316 data

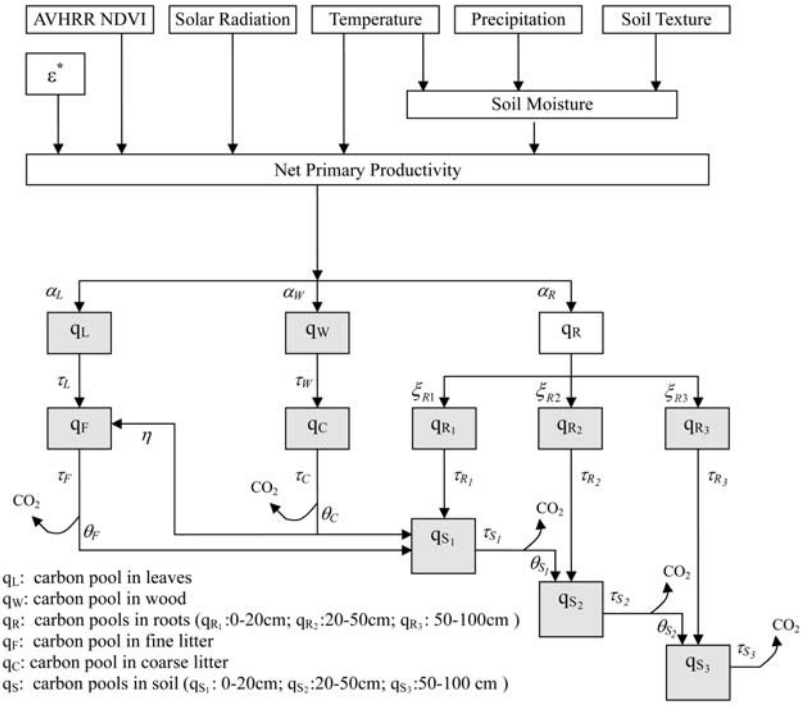

Figure 1. Terrestrial Ecosystem Regional (TECO-R) model structure for inversion analysis of carbon residence times. Net primary production (NPP) is modeled by the light-use efficiency model (Carnegie-Ames-Stanford-Approach (CASA)), and it allocated to plant tissues (leaf q_L, stem q_W, and root q_{Rj}) on the basis of allocation coefficients (α_L, α_W, α_R). Plant tissues enter into fine litter (q_F), coarse litter (q_C), and soil organic carbon pools (q_s) through litterfall. Decomposed litter releases part of the carbon to the atmosphere, and the rest transfers into the soil (θ_C, θ_F). Through mechanical breakdown, part of the coarse litter becomes fine litter (η). To reflect the differences in soil profile, roots and soil organic carbon pools are divided into three layers (top: 0–20 cm, middle: 20–50 cm, and bottom: 50–100 cm).

Table 1. Symbol and Definition of Parameters, Their Lower and Upper Limits, and Other Constraints for Inverse Analysis[a]

Symbol	Definition	LL	UL	Other Constraint
ε^*	Maximum light-use efficiency	0.0	2.76	
α_L	Allocation of NPP to leaves	0.0	1.0	$\alpha_L > \alpha_W$
α_W	Allocation of NPP to wood	0.0	1.0	$\alpha_W = 0$ for grassland and cropland
α_R	Allocation of NPP to roots	0.0	1.0	$\alpha_L + \alpha_W + \alpha_R = 1$
ξ_{R1}	Allocation proportion of NPP for roots (0–20 cm)	0.0	1.0	$\xi_{R1} > \xi_{R2} > \xi_{R3}$
ξ_{R2}	Allocation proportion of NPP for roots (20–50 cm)	0.0	1.0	
ξ_{R3}	Allocation proportion of NPP for roots (50–100 cm)	0.0	1.0	$\xi_{R1} + \xi_{R2} + \xi_{R3} = 1$
θ_F	Carbon partitioning coefficient of the fine litter pool	0.0	0.5	
θ_C	Carbon partitioning coefficient of coarse litter pool	0.0	0.5	$\theta_C = 0$ for grassland and cropland
θ_{S1}	Carbon partitioning coefficient of SOC (0–20 cm)	0.0	0.1	
θ_{S2}	Carbon partitioning coefficient of SOC (20–50 cm)	0.0	0.1	
η	Fraction of mechanical breakdown for coarse litter pool	0.0	0.1	
τ_L	Site specific carbon residence time of leaves	0.0	10.0	$0 \le \tau_L \le 1$ for deciduous broadleaf forest
τ_W	Site specific carbon residence time of wood	0.0	500.0	$\tau_W > \tau_L$, not for grassland and cropland
τ_{R1}	Site specific carbon residence time of roots (0–20 cm)	0.0	10.0	$\tau_{R1} < \tau_{R2} < \tau_{R3}$
τ_{R2}	Site specific carbon residence time of roots (20–50 cm)	0.0	20.0	$\tau_{R2} \le 5$ for grassland and cropland
τ_{R3}	Site specific carbon residence time of roots (50–100 cm)	0.0	50.0	$\tau_{R3} \le 5$ for grassland and cropland
τ_F^*	Moisture and temperature corrected residence time of fine litter	0.0	10.0	
τ_C^*	Moisture and temperature corrected residence time of coarse litter	0.0	50.0	$\tau_C^* > \tau_F^*$, not for grassland and cropland
τ_{S1}^*	Moisture and temperature corrected residence time of SOC (0–20 cm)	0.0	100.0	$\tau_{S1}^* < \tau_{S2}^* < \tau_{S3}^*$
τ_{S2}^*	Moisture and temperature corrected residence time of SOC (20–50 cm)	0.0	250.0	
τ_{S3}^*	Moisture and temperature corrected residence time of SOC (50–100 cm)	0.0	500.0	

[a]Units are gC MJ^{-1} PAR for ε^* and years for residence times. Allocation and partitioning coefficients are dimensionless. LL: lower limits; UL: upper limits; SOC: soil organic carbon; NPP: net primary production.

points in biomass, and 6869 data points in SOC. Spatial distribution of the data points and the detailed information of data points and their sources are listed in Figure S1 and Text S1.[1]

[11] Sources of auxiliary data used in this study were (1) the AVHRR-NDVI continental subsets of 8-km spatial resolution from 1982 to 1999 available from the Data and Information Services Center of Goddard Earth Science; (2) annual solar radiation produced by the NASA/Global Energy and Water Cycle Experiment with one-by-one degree spatial resolution; (3) monthly precipitation and temperature data sets with 4-km spatial resolution offered by the Spatial Climate Analysis Service; (4) soil texture data set from State Soil Geographic Database (STATSGO) available from USDA Natural Resources Conservation Service; and (5) 1-km spatial resolution land cover data, containing eight vegetation types in the conterminous United States, derived from AVHRR using a decision tree classifier [*Hansen et al.*, 2000]. All those auxiliary data sets were resampled to a common projection (Lat-Long Projection) and spatial resolution (0.04 degree).

2.2. Parameter Estimation

[12] The parameter estimation was based on the weighed least squares principle that minimized the deviations between the modeled and observed values of all the 12 data sets for each of the eight biomes, which included evergreen needleleaf forest (ENF), deciduous broadleaf forest (DBR), mixed forest (MF), woodland (W), wooded grassland (WG), shrubland (S), grassland (G), and cropland (C). Given one biome, we defined a partial cost function j_m as the sum of squares of deviations between observed and modeled values for data set m:

$$j_m = \sum_{n=1}^{N_m} [y_{nm} - \hat{y}_{nm}(x_n, \mathbf{a})]^2 \tag{1}$$

where y_{nm} is the nth observed data point in the mth data set; $\hat{y}_{nm}(x_n; \mathbf{a})$ is the modeled value that corresponds to the observation y_{nm}; N_m is the total data points in the mth data set; x_n is an auxiliary forcing vector that includes NDVI, solar radiation, air temperature, precipitation, and soil texture, in a spatial grid where the nth observation was made; and a is a vector consisting of 22 parameters: $\mathbf{a} = \{\varepsilon^*, \alpha_L, \alpha_W, \alpha_R, \xi_{R1}, \xi_{R2}, \xi_{R3}, \tau_L, \tau_W, \theta_F, \theta_C, \eta, \tau_{R1}, \tau_{R2}, \tau_{R3}, \tau_F^*, \tau_C^*, \tau_{S1}^*, \tau_{S2}^*, \tau_{S3}^*, \theta_{S1}, \theta_{S2}\}$. Each of the parameters is described with equations in Appendix A and also defined in Table 1.

[13] A particular data set may provide information to constrain a subset of parameters in vector **a**. For example, the data set of leaf NPP directly constrains the parameters of ε^*, α_L, and τ_L. When all 12 data sets are used, all 22 parameters can be constrained to a certain degree. One parameter may be constrained by multiple data sets. In this case, an integrated cost function J, which consists of M (=12) partial cost functions j_m, is defined to measure the deviations between modeled and observed values for all the data points in the 12 data sets. Thus the cost function, J, to be minimized is

$$J = \sum_{m=1}^{M} \lambda_m \left\{ \sum_{n=1}^{N_m} [y_{nm} - \hat{y}_{nm}(x_n, \mathbf{a})]^2 \right\}, \qquad m = 1, 2, \ldots, M \tag{2}$$

where λ_m is a weighing factor of the partial cost j_m, which is inversely proportional to the variance of each data set. Thus, each data set was equally weighed in the cost function [*Luo et al.*, 2003]. The cost function, J, in equation (2) was applied to each of the eight biomes so that eight sets of biome-specific values of parameter vector, **a**, were obtained in this study.

[14] To estimate the globally optimal parameters, the genetic algorithm (GA) was used in this study. The parameter spaces and constraints shown in Table 1 were defined primarily in reference to the work by *Barrett* [2002], but specified for their applications to eight vegetation types in this study instead of three biomes in the continent of Australia. The steps of searching for the globally optimal parameters in this study were (1) initializing the parameter vector, **a**, from the parameter ranges in Table 1 with random numbers; (2) applying genetic algorithm (selection, crossover, and mutation) to generate the new offspring of parameter values of **a**; (3) using the generated parameter values in equations (A5)–(A11) to calculate the modeled value, $\hat{y}_{nm}(x_n; \mathbf{a})$, under a steady state assumption (i.e., the $dq_i/dt = 0$, i = L, W, R1, R2, R3, F, C, S1, S2, and S3); (4) using observation data, y_{nm}, and corresponding modeled value, $y_{nm}(x_n; \mathbf{a})$, to calculate partial cost function, j_m, in equation (1); (5) calculating integrated cost function J; and (6) judging stopping condition of evolution (change of J in last 100 offspring less than 0.01%). If the stopping criterion was satisfied, then the algorithm exported the optimal parameters. Otherwise it went to step (2) to continue the search.

[15] The estimated C residence times and allocation coefficients for individual C pools in plants and soils were used to calculate the aggregated C residence time for the whole ecosystem τ_E using the following formula [*Barrett*, 2002]:

$$\begin{aligned}\tau_E = {} & \alpha_L(\tau_L + \tau_F) + \eta\alpha_W\tau_F + \alpha_W(\tau_W + \tau_C) \\ & + \alpha_R\left[\xi_{R_1}(\tau_{R_1} + \tau_{S_1}) + \xi_{R_2}(\tau_{R_2} + \tau_{S_2}) + \xi_{R_3}(\tau_{R_3} + \tau_{S_3})\right] \\ & + F_1\tau_{S_1} + F_2\theta_{S_1}\tau_{S_2} + F_3\theta_{S_2}\tau_{S_3}\end{aligned} \tag{3}$$

where

$$\begin{aligned}F_1 &= \theta_F(\alpha_L + \eta\alpha_W) + \theta_C\alpha_W \\ F_2 &= \alpha_R\xi_{R_1} + F_1 \\ F_3 &= \alpha_R\xi_{R_2} + \theta_{S_1}F_2\end{aligned} \tag{4}$$

[16] We have run the optimization algorithm for 30 times to obtain means and standard errors of the estimated parameters. Estimated standard errors reflected integration

[1] Auxiliary materials are available in the HTML. doi:10.1029/2007GB002939.

of model errors, data errors, and errors in the data-model fusion technique.

2.3. Carbon Uptake

[17] The means of parameter values estimated from genetic algorithms together with the corresponding carbon pool sizes in the inverse analysis were used in forward modeling to simulate carbon uptake. The same set of environmental variables (e.g., temperature, precipitation, land cover, and soil texture) used in the inverse analysis was used in the simulation of carbon uptake.

[18] We applied the NPP increase trend estimated by *Hicke et al.* [2002] to quantify spatial distributions of carbon uptake in the conterminous United States in two ways. One was that an assumed uniform NPP increase, 1.83 g C m^{-2} a^{-1} (i.e., the averaged NPP increase in the conterminous United States estimated by *Hicke et al.* [2002]), was used for each spatial grid to evaluate C uptake. So, the spatial difference of C uptake potential in this case was caused only by the spatial pattern of C residence times. The other case was that the actual spatial pattern of NPP increases [*Hicke et al.*, 2002], combined with the spatial pattern of C residence times, was used as the driving forces to evaluate the actual C uptake potential caused by both NPP increases and C residence times. The two ways of evaluating carbon uptake can help distinguish roles of NPP increase and residence times in regulation of C uptake. The NPP increase trend was a direct driving force as it induced more C (extra carbon) to enter into the ecosystem. Carbon residence times determined the length of time the extra carbon can stay in the ecosystem and then regulated the capacity of C uptake in the ecosystem [*Luo et al.*, 2001, 2003].

[19] To focus on these two factors of NPP increases and C residence times in influencing C uptake, we assumed that there were no changes in other environmental factors (e.g., temperature) and the same rate of NPP change continued for 50 years.

2.4. Sensitivity Analysis

[20] Sensitivity analyses were conducted to evaluate impacts of observation errors, steady state assumption, and initial soil organic C on parameter estimation and on the C uptake. Because of the lack of well-documented time serials of data on NPP, plant biomass, and SOC in most of the ecosystems, this study was unable to estimate residence times and initial values of pool sizes to assess nonsteady state carbon dynamics as done by *White et al.* [2005]. To examine influences of the steady state assumption on the estimated residence times, we conducted a sensitivity analysis to estimate nonsteady state carbon residence times. In the analysis, we increased C influx into an ecosystem so that C uptake equals 10 to 50% of NPP ($\overline{NPP}$). That is, the yearly C uptake equals 0.1 $\overline{NPP}$, 0.2 $\overline{NPP}$, 0.3 $\overline{NPP}$, 0.4 $\overline{NPP}$, and 0.5 $\overline{NPP}$, respectively. Under these nonsteady state scenarios, the C residence times were estimated and compared with those under steady state.

[21] As measurement errors in the observed data sets potentially impact the precision of the estimated parameters in the inverse analysis [*Raupach et al.*, 2005], we conducted a sensitivity analysis to assess the sensitivity of the estimated parameters to measurement errors. Eight scenarios were used in this study; each scenario assumed only one observation data set being overestimated and underestimated by 20%, respectively. The observation data sets in eight scenarios included (1) leaf NPP; (2) stem NPP; (3) root NPP; (4) leaf biomass; (5) stem biomass; (6) SOC in layer 1 (0–20 cm); (7) SOC in layer 2 (20–50 cm); and (8) SOC in layer 3 (50–100 cm).

[22] Land use change can substantially influence carbon uptake. We did a sensitivity analysis to evaluate potential impacts of land use on parameter estimation. We decreased soil organic carbon by 40% for the woodland to simulate land use change from previous croplands and increased it by 40% for cropland to simulate land use change from previously forested lands.

[23] Another factor that influences soil C uptake is the initial value of SOC content when C cycling processes were not in steady state. We did a sensitivity analysis to assess effects of initial values on parameter estimation with three scenarios: initial SOC being 20% below, at, and 20% above the equilibrium level.

3. Results

3.1. Comparisons Between Modeled and Observed Data Sets

[24] Comparisons between modeled and observed data sets are important to evaluate the validity of the inverse analysis method. The searching process for the best parameters (shown in Figure S2) shows that the genetic algorithm was effective in this study; all the best parameters were obtained in 100,000 trials. With the best parameters in the model, the modeled values were closely related to the corresponding observed data (Figure 2). There were a few cases where modeled values deviated from observations. For example, modeled NPP in stem was lower than the observed values, probably because of correlative relationships between parameters of carbon partitioning and residence time. The tradeoff of estimated parameter values under the integrated cost function J (equation (2)) minimized the total deviation for all data sets possibly at expense of stem NPP.

3.2. Estimated Carbon Allocation Coefficients and Light-Use Efficiencies

[25] Allocation coefficients of NPP to leaves, stem, and roots estimated from this inverse analysis varied with biome types (Figure 3). The evergreen needleleaf forest, deciduous broadleaf forest, and woodland had similar C allocation coefficients for leaves (33–37%), wood (33–37%), and roots (26–34%). The mixed forest had higher C allocation for leaves and wood (40%) and accordingly lower allocation for roots (20%). The wooded grassland had relatively higher C allocation for roots (38%), compared with the other forests and woodland. The shrubland and grassland had the highest C allocation for roots (56–58%). Although both the grassland and cropland allocated C only between leaves and roots, the grassland allocated much more C to roots (58%) than the cropland does (24%). This is consistent with

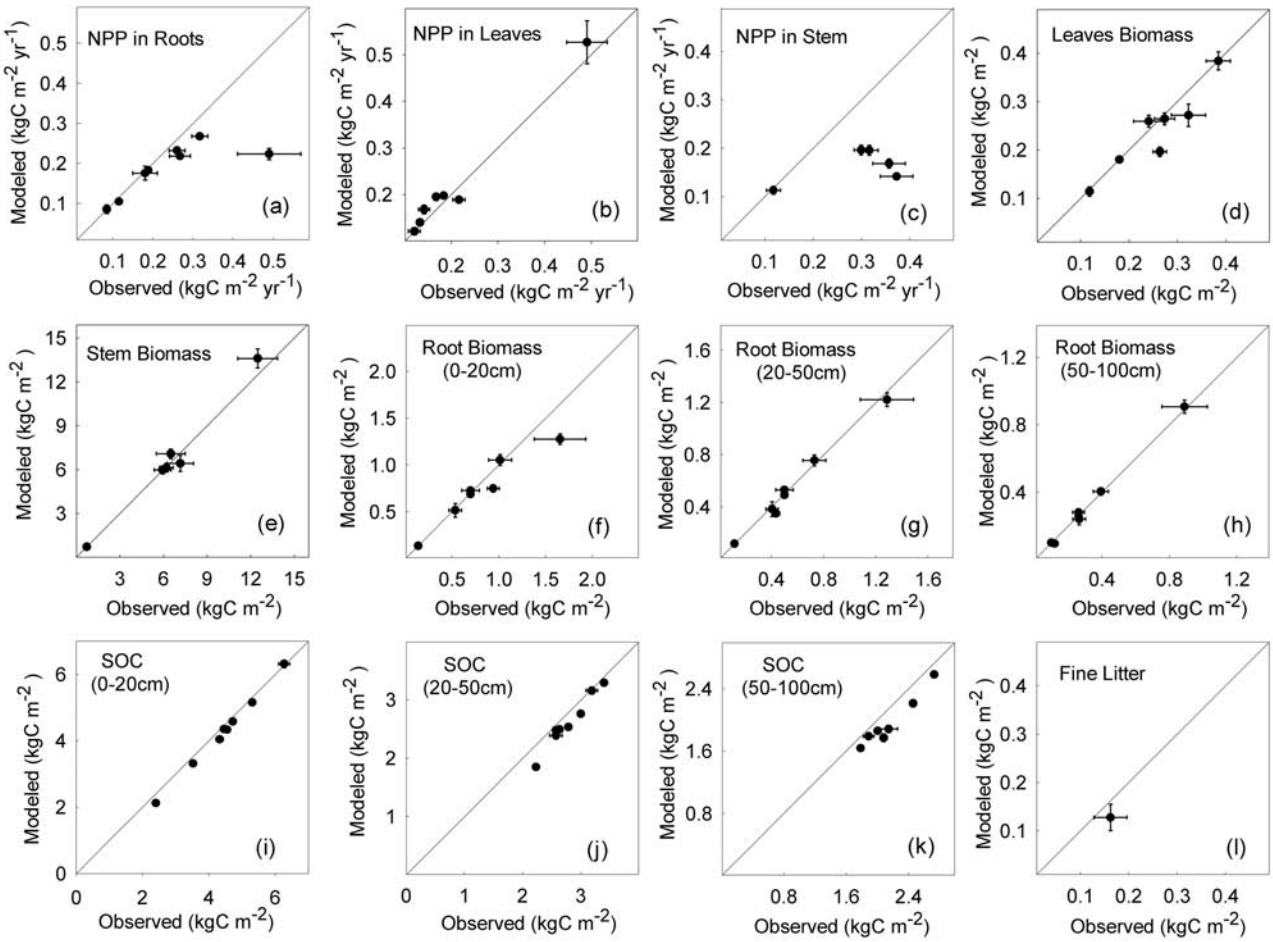

Figure 2. Comparisons between modeled and observed values of NPP, biomass, fine litter, and soil organic carbon (SOC) in eight biomes. Points in each panel represents means of biomes with horizontal and vertical standard error bars to indicate variations among observed and modeled values, respectively. Overall, modeled NPP, biomass, fine litter, and SOC are highly correlated with observed ones. Some panels do not have eight data points because of the lack of observations in some of the biomes.

results from *Bradford et al.* [2005], who found that the cropland allocated 28% of NPP to roots, much lower than the grassland.

[26] The estimated maximum potential light-use efficiencies (ε*) of the deciduous broadleaf forest, mixed forest, and woodland were similar, with values of 0.43 to 0.49 g C MJ^{-1} PAR (Figure 3). The wooded grassland had higher light-use efficiency (0.55) than the evergreen needleleaf forest and shrubland (0.36 and 0.28, respectively). Compared to the forests and woodlands, the grassland and cropland had relatively high light-use efficiencies of 0.56 and 0.93, respectively. Our estimated light-use efficiency of cropland was at the upper end of the range from 0.41 to 0.94 g C MJ^{-1} PAR given by *Lobell et al.* [2002].

3.3. Estimated Carbon Residence Times in Plant Biomass, Litter, and Soil Pools

[27] The residence times of aboveground biomass pools estimated from this inverse analysis were from 1.0 to 2.03 years for leaves (τ_L) and from 30.7 to 49.7 years for wood (τ_W) among the deciduous broadleaf forest, mixed forest, woodland, and wooded grassland. Leaves and wood of the evergreen needleleaf forest and shrubland had longer residence times, ranging from 2.73 to 3.90 years for leaves and from 96.7 to 109.0 years for wood. The root residence times were 6.78–9.98 years in the topsoil layer and 9.19–19.6 years in the middle soil layer for the forests, woodland, and shrubland. The root residence times in the bottom soil layer were longer than those at the top and middle layers. The residence times for leaves in the grassland and cropland were 0.59 and 0.26 years, respectively, smaller than those for the forests and woodlands. Root residence times for the grassland and cropland did not vary much along soil profiles.

[28] The temperature- and moisture-corrected C residence times (τ_k*) for litter and SOC in the different biomes were plotted in Figure 3. The estimated C residence times values for fine litter (τ_F*) were 0.83 to 0.94 years for all the forests and woodlands. The grassland had the lowest value (τ_F* = 0.17). The residence times for coarse litter (τ_C*) ranged

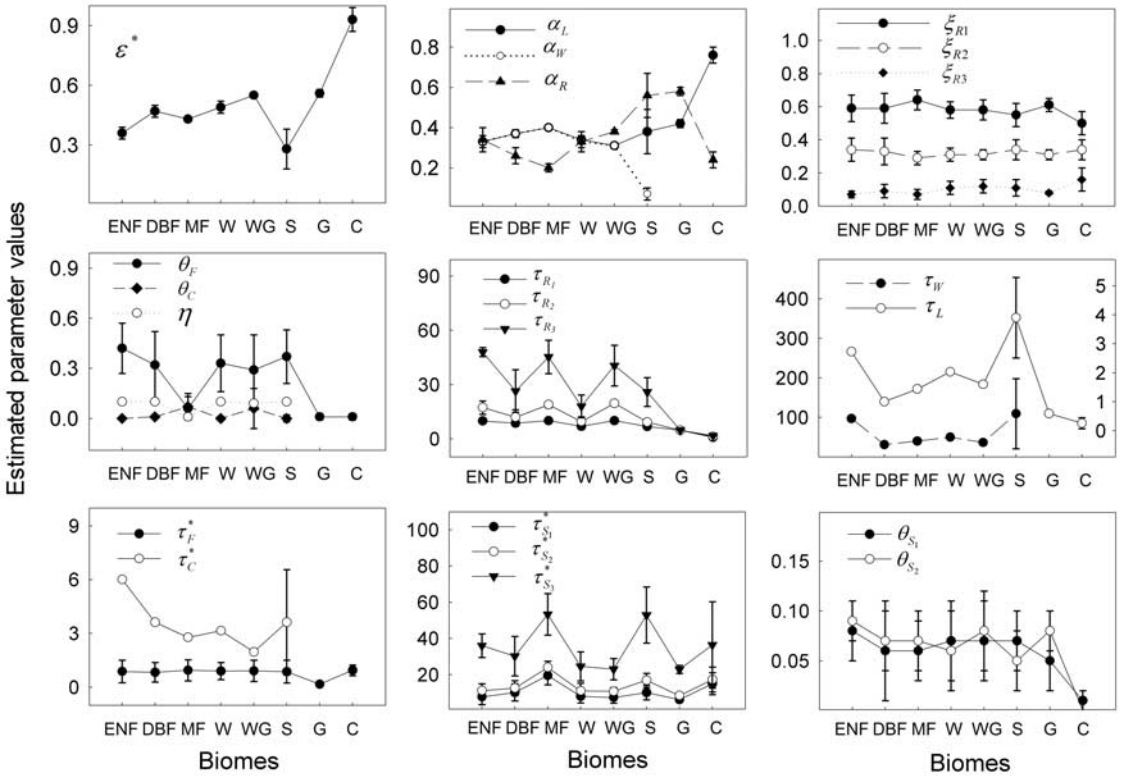

Figure 3. Optimized values of 22 parameters for eight biomes with mean ±one standard deviation of optimized values from 30 runs of genetic algorithm. Symbols for the 22 parameters are described in Table 1.

from 1.97 to 6.01 years. The values of SOC (τ_{S1}*,τ_{S2}*,τ_{S3}*) were much higher than those for litters, ranging from 6.19 to 19.6 years for the topsoil layer, from 8.47 to 24.0 years for the middle layer, and from 22.9 to 53.3 years for the bottom layer. Among the eight biomes, the mixed forest had the highest residence times for SOC in all three layers, whereas the grassland had the lowest residence times for SOC.

[29] Because of spatial heterogeneities of temperature and moisture, the actual residence times of litter and soil (τ_k) were different fromτ_k*. The values of τ_k ranged from about 1 to 4 years for fine litter, with the minimum for the grassland and the maximum for the evergreen needleleaf forest and shrubland. The actual residence times for coarse litter ranged from 5 years for the wooded grassland to 24 years for the evergreen needleleaf. The τ_k values ranged from 26 to 77, from 32 to 102, and from 63 to 195 years, respectively, for SOC in the three soil layers, much larger than the corresponding temperature- and moisture-corrected τ_k* values.

3.4. Spatial Patterns of Ecosystem Residence Times

[30] The C residence times of the whole ecosystem in the conterminous United States were highly heterogeneous, ranging from 10 years in some cropland grids to 150 years in some shrubland grids. However, the residence times in most grids were between 15 and 65 years (Figure 4). The central Great Plains had the lowest residence times and the west regions had the highest values, with the east regions in middle. The averaged C residence time of the whole conterminous United States was 46 years.

[31] The forest, woodland, and shrubland had higher residence times than the grassland and cropland. Within the entire conterminous United States, the evergreen needleleaf forest had the highest residence time of 85 years, because of low temperature in its habitat. The shrubland also had a high residence time of 67 years because of the dry conditions in its habitat. The cropland and grassland had the lowest residence times (19 and 29 years) because of the lack of long-residence wood tissues and litter. The other biomes had residence times between 36 and 50 years.

3.5. Carbon Uptake in Ecosystems

[32] When the assumed uniform NPP increase of 1.83 g C m^{-2} a^{-1} (i.e., the averaged NPP increase at the conterminous United States) was applied to each spatial grid, east and west regions had relatively higher C uptake, with the values ranging from 23 to 38 g C m^{-2} a^{-1} (Figure 5a). The estimated C uptake in the center regions was relatively smaller, with the values ranging from 14 to 23 g C m^{-2} a^{-1}. As the magnitude of NPP increase was the same for each spatial grid under the assumed uniform NPP increase, the differences of C uptake in Figure 5a reflected spatial differences in the ecosystem C residence times (Figure 4). Thus, the residence times determined the fraction of influx C uptaked.

[33] Modeled soil C uptake (Figure 5b) under the assumed uniform NPP increase shows that grassland, shrub-

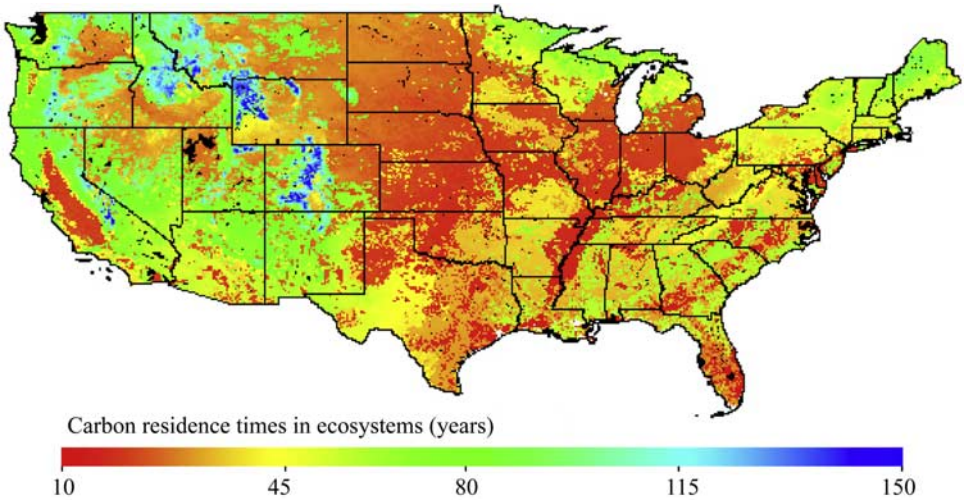

Figure 4. Spatial patterns of ecosystem carbon residence times estimated by inverse modeling for the conterminous United States. Estimated residence times are high in Rocky Mountain alpine and northern forest regions but low in croplands in the Great Plains.

land, and cropland had apparently higher percentages of C uptaked in soils, whereas forests and woodlands tended to uptake lower percentage of C in soils (about 20%). The spatial pattern of percent soil C uptake was controlled by the residence times of soil C pools (Figure 3) and their relative C allocation coefficients of NPP to roots, leaves, and stems.

[34] When the actual, spatially heterogeneous NPP increases [*Hicke et al.*, 2002] were used in the forward modeling, the spatial patterns of the estimated ecosystem C uptake (Figure 5c) were quite different from Figure 5a. The southeast region had higher C uptake, because of the relatively higher values of both NPP increase and carbon residence times (Figure 4). The fact that the central Plains had higher C uptake was mainly attributed to the highest NPP increase in the conterminous United States. Some

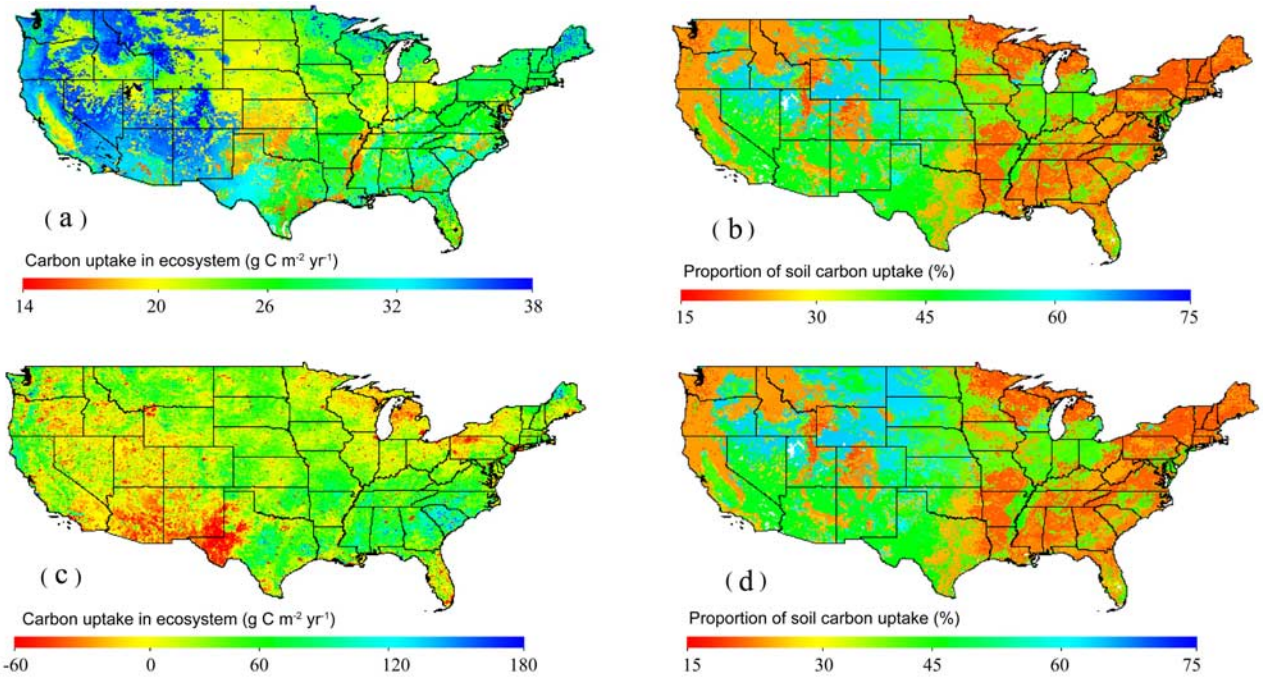

Figure 5. Ecosystem carbon uptakes driven by NPP increases. (a, b) Ecosystem carbon uptake and proportions of soil carbon uptake, respectively, driven by an assumed uniform NPP increase. (c, d) Ecosystem carbon uptake and proportions of soil carbon uptake, respectively, driven by the actual spatially heterogeneous NPP increases [*Hicke et al.*, 2002].

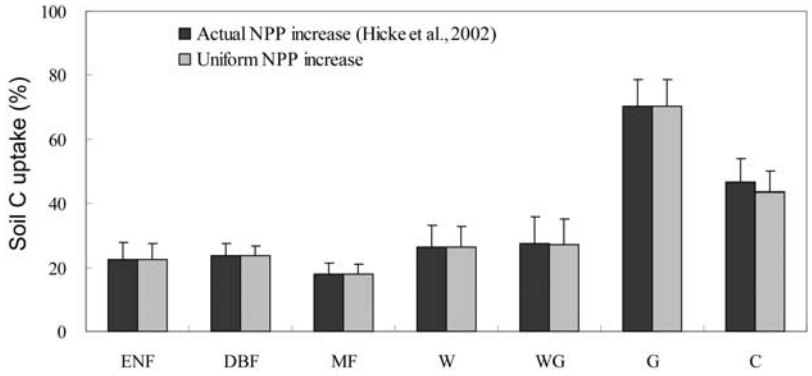

Figure 6. Proportions of soil C uptake for different biomes with either uniform or actual NPP increases. Although ecosystem C uptake varies with the two scenarios of NPP increases, the proportions of net C uptake to be stored in soil are almost identical among biomes.

southwest regions had negative C uptake because of decreased NPP during the period.

[35] Although the rate of NPP increase impacted ecosystem C uptake (Figures 5a and 5c) and then induced differences in magnitude for soil C uptake between the assumed uniform NPP increase and the actual spatially heterogeneous NPP increase, the proportions of C uptake in soil relative to the total C uptake in the ecosystem were nearly invariable (Figures 5b and 5d). That means that the proportions of soil C uptake were mainly controlled by C residence times and independent of the rate of the NPP increase. On the biome scale, grassland and cropland had relatively higher proportions of soil C uptake (47–70%) than did forests and woodlands (18–27%) (Figure 6).

[36] Integration of the spatial patterns of both the NPP increase and C residence times shows that the ecosystems of the conterminous United States were a C sink. Their averaged C uptake was 19.91g C m^{-2} a^{-1}, and the total C uptake was 0.15 Pg C per year, about one third (38%) of which was stored in soil.

3.6. Sensitivity Analysis

[37] When the magnitude of carbon uptake varied from 10 to 50% of the total NPP, the estimated residence times increased by 4.7–42.4% (Figure 7). Thus, the steady state assumption resulted in underestimation of residence times when ecosystems were C sink. The magnitude of C sink was usually around 5% of cumulative C input via NPP increases except in regions where land use change or other disturbances had dramatically altered C balance. Thus, the influence of this steady state assumption was not substantial.

[38] When NPP, biomass, and SOC increased or decreased by 20%, the cost function, J, and the majority of the parameters did not change much (usually, <5%) (Figure 8). That means the estimation of most parameters by this inversion method was relatively robust. Nevertheless, the allocation coefficient (α_L) and residence time for leaves (τ_L) were somewhat sensitive to changes in leaf NPP. When leaf and stem biomass increased or decreased by 20%, residence times for leaves (τ_L) and wood (τ_W) varied by more than 20% in the corresponding directions. Simi-

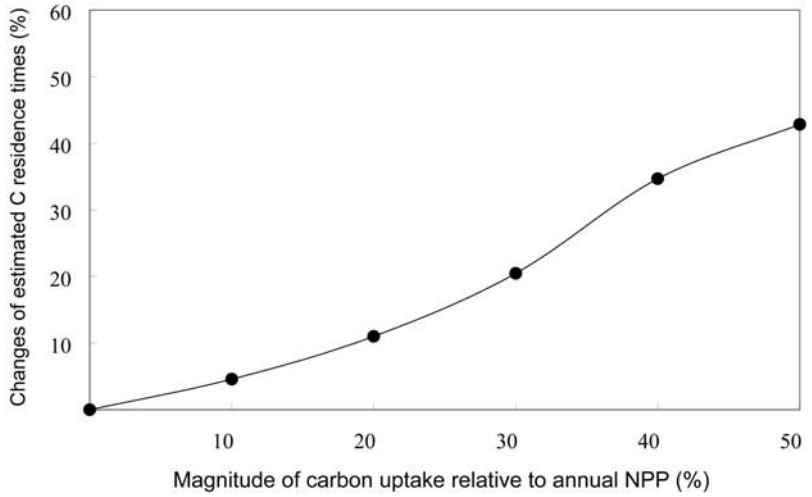

Figure 7. Sensitivity analysis of the estimated C residence times in nonsteady state. Estimated C residence times increase as the magnitude of carbon uptake varied from 10 to 50% of the total NPP.

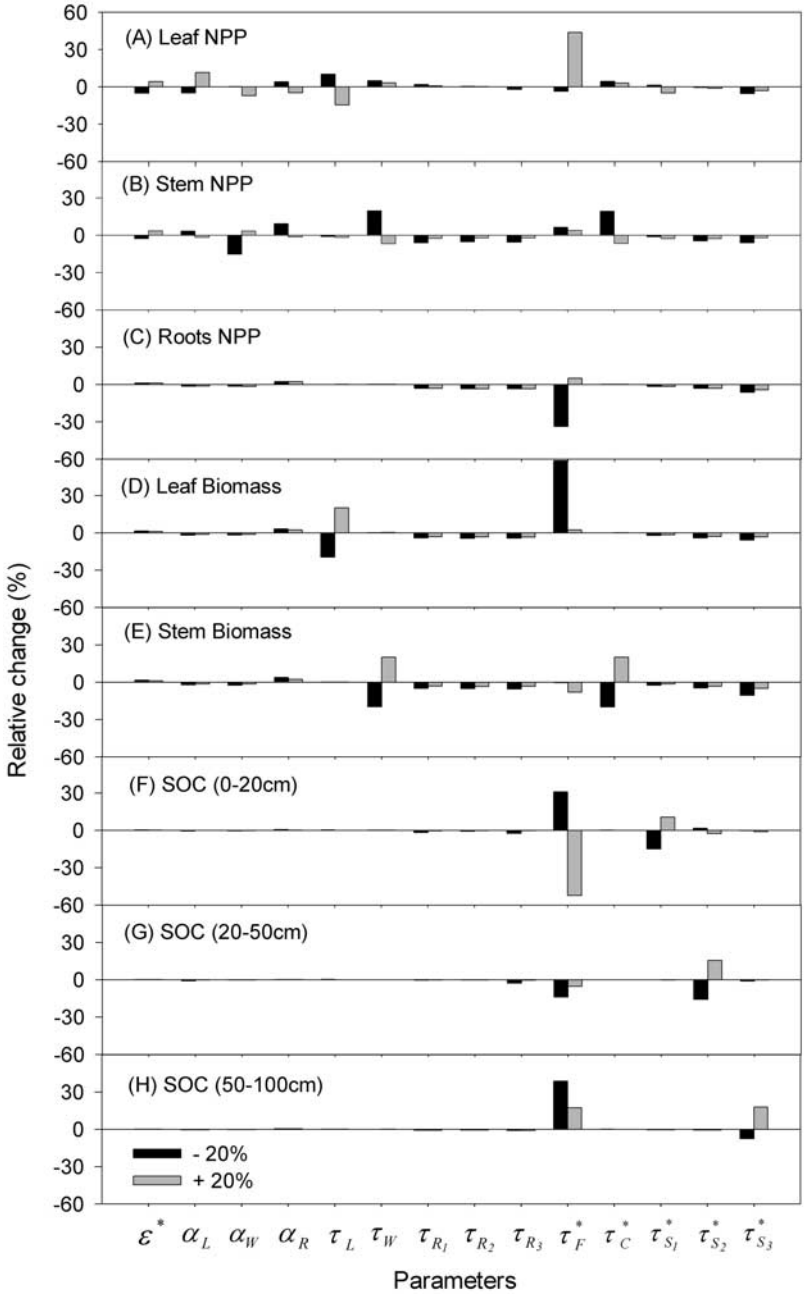

Figure 8. Sensitivity analyses on estimated parameters as eight sets of observed data, which are (a) leaf NPP; (b) stem NPP; (c) root NPP; (d) leaf biomass; (e) stem biomass; (f) SOC in layer 1 (0–20 cm); (g) SOC in layer 2 (20–50 cm); and (h) SOC in layer 3 (50–100 cm), varied by ±20%. Note that cost function J and parameters ξ_{R1}, ξ_{R2}, and ξ_{R3} were not plotted here because they did not vary much in response to changes in the eight sets of observed data.

larly, residence times for SOC (τ_s*) were sensitive to changes in SOC.

[39] When data that are directly related to the parameter were not available, the residence time of fine litter (τ_F*) was sensitive to variations in observed values of all eight data sets tested in this study and changed up to 50% in response to a 20% increase in leaf biomass (Figure 8). In addition, variations in leaf NPP data by 20% strongly affected not only the parameters that are directly related to this data set (e.g., ε*, α_L, α_W, α_R) but also downstream parameters along C transfer processes (i.e., litter and SOC). In contrast, variations in SOC data by 20% hardly affected upstream parameters along C transfer processes.

[40] When observed SOC values decreased by 40% for the woodland and increased by 40% for cropland, inverted coefficients and residence times in plant and litter pools did

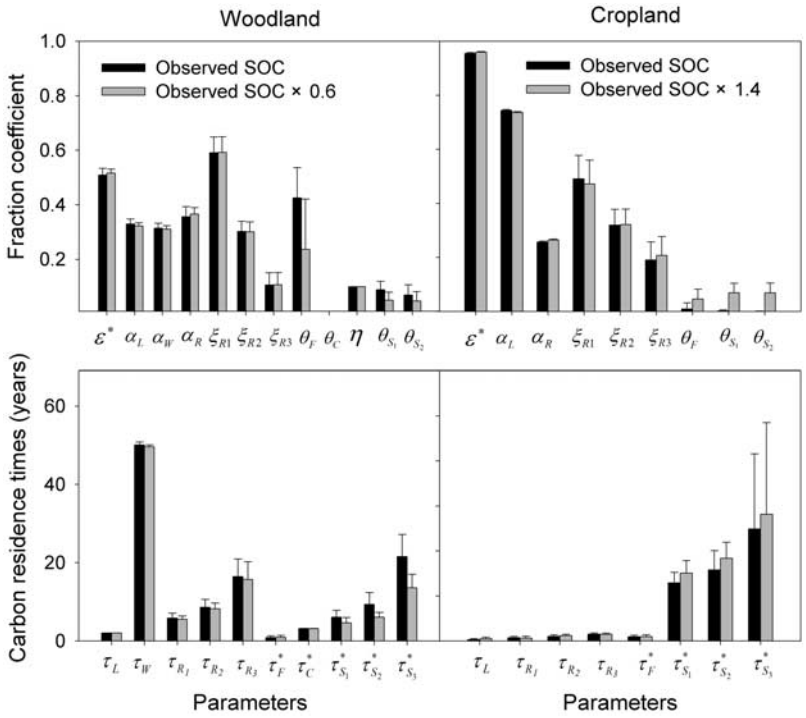

Figure 9. Sensitivity analysis for simulating land use change on parameter estimation with SOC in woodland decreasing by 40% and SOC in cropland increasing by 40%.

not change much (Figure 9). The inverted soil residence times (τ_{S1}*, τ_{S2}*, and τ_{S3}*) and carbon partitioning coefficients of SOC (θ_{S1}, θ_{S2}) among soil carbon pools decreased by 20–40% in response to a 40% decrease in SOC in the woodland but increased in a similar magnitude with the opposite direction in response to a 40% increase in SOC in the cropland.

[41] The lower the initial SOC, the higher the rate of carbon uptake was in soil under the same driving of NPP increase (Figure 10). The soil carbon uptake was 24.06, 6.56, and −10.94 g C m^{-2} a^{-1}, respectively, when initial SOC at the beginning of simulation was 20% below, at, and 20% above the equilibrium level.

4. Discussions

4.1. Carbon Residence Times

[42] Our estimated C residence times of leaves for forests and woodland ranged from 1.0 to 2.73 years. As comparison, observation-based residence times (i.e., ratios of observed stock divided by observed flux) are 1.64 years for woodland [*DeAngelis et al.*, 1997] and 2.32 years for forest [*Cannell*, 1982]. The estimated residence time of leaves was 0.59 years for grassland, which is very comparable with the observation-based 0.50 years [*Turner*, 1994; *Scurlock et al.*, 2003]. Except for the evergreen needleleaf forest, the woods of forests and woodlands had residence times of 30.7–49.7 years, similar to the observation-based values [*DeAngelis et al.*, 1997; *Cannell*, 1982]. The estimated residence times for forest and woodland roots at the depth from 0 to 100 cm ranged from 11 to 18 years, which were in the low end of the observation-based 18–23 years [*DeAngelis et al.*, 1997; *Cannell*, 1982]. Our estimation of temperature-dependent residence time of fine litter (τ_F) was 0.77 years, slightly higher than the observation-based 0.51 years [*Scurlock et al.*, 2003].

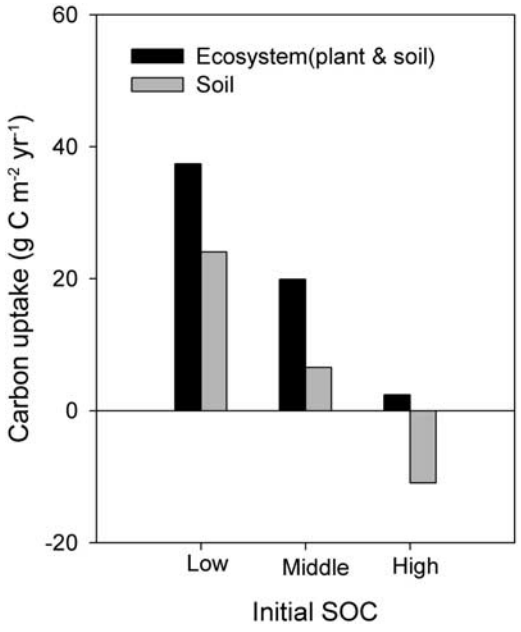

Figure 10. Sensitivity analysis of carbon uptake caused by different initial SOC contents of 20% below (low), at (middle), and 20% above (high) the equilibrium level.

[43] The inverse of temperature-dependent residence time of coarse litter is the decomposition constant (usually so-called k value). The k value of this study was 0.05 for the evergreen needleleaf forest, 0.08 for the deciduous broadleaf forest, 0.10 for the mixed forest and woodland, 0.20 for the wooded grassland, and 0.12 for the shrubland. These k values are consistent with the estimations that derived from wood decomposition experiments. For example, *Todd and Hanson* [2003] summarized the k values of coarse-wood decomposition for deciduous and coniferous species of the eastern United States and indicated that the k values ranged from 0.03 to 0.43. The estimated k value for fine litter in this study was about 1.06–1.20, very similar to the mean values from meta-analyses by *Silver and Miya* [2001] and *Zhang et al.* [2008].

[44] Consistencies between our estimated residence times through inverse analysis and observation-based values and between modeled and observed data in Figure 2 suggested the validity of the inversion approach to estimation of C residence times. The inversion approach is advantageous over the observation approach in that not only did it reveal the parameters that can be observed through experiments but also parameters that are not observable or difficult to observe from experiments, such as residence times of root or SOC. In addition, the estimated residence times in different C pools from the inverse analysis can be used to characterize the whole ecosystem C dynamics.

4.2. Carbon Uptake

[45] Total C uptake driven by NPP changes in the conterminous United States was estimated to be 0.15 Pg C a^{-1}. This value is comparable with the estimate of 0.15–0.35 Pg C a^{-1} based on the analysis of historical data on land use and land cover changes by *Houghton et al.* [1999]. Our estimation of the continental C sink is larger than the modeled value of 0.08 Pg C a^{-1} conducted by the VEMAP study [*Schimel et al.*, 2000]. The estimation of carbon sink by atmospheric inversion suggested a relatively higher carbon sink (0.30∼0.58 Pg C a^{-1}) [*Pacala et al.*, 2001] than our estimate probably because carbon export of 0.11 to 0.24 Pg C a^{-1} by rivers was contained in the atmospheric inversion but not accounted for in terrestrial ecosystem models and inventory surveys.

[46] The study shows that both forest and nonforest ecosystems were important for C uptake in the conterminous United States. The most important forests for C uptake were located in the southeast regions (Figure 5c). This study indicates that grasslands and croplands in Great Plains also uptaked substantial amounts of C (Figure 5c). This result was similar to the estimation by atmospheric inverse analysis that about one half of the total C uptake in the United States continent was outside the forest sector [*Pacala et al.*, 2001]. As croplands had the highest increasing trend in NPP [*Hicke et al.*, 2002], and the largest area (23% of total area in the conterminous United States), C uptake in croplands was very important (Figure 5c).

[47] The parameters of C residence times and allocation coefficients are very important in determining how the uptaked C is distributed among various pools [*Post et al.*, 2004]. Our study showed that the forests and woodland stored 18% to 27% of uptaked C in soils (Figure 6), which was consistent with the forest inventory. For example, *Goodale et al.* [2002] used the forest inventory data from more than 42 countries to analyze forest C sinks in the Northern Hemisphere. They found that the total sink in the entire forest ecosystem in the Northern Hemisphere was 0.6–0.7 Pg C a^{-1}, of which the soil sink was 0.13 Pg C a^{-1} (accounting for about 20% of the total sink). Similarly, the European forests survey showed that forests (both trees and soil) uptaked 0.117 Pg C a^{-1}, of which 0.023 Pg C a^{-1} (i.e., 19.7%) was uptaked in soil [*de Vries et al.*, 2006]. Plant biomass stored most of the uptaked C in the forests and woodlands because of relatively high C allocation coefficients for woods (Figure 3) with high C residence times (Figure 4). In contrast, grasslands and croplands stored the majority of uptaked C in soils (Figure 6) because of relatively small amounts of biomass with long C residence times.

[48] Terrestrial carbon sink can be attributable to a variety of mechanisms, such as CO_2 fertilization, N-fertilization, forest regrowth, intensive crop and forest management practices, and any recovery from prior land use change and disturbances. The carbon uptake in the central Plains, for example, could be a result of intensive crop management [*Lobell et al.*, 2002]. The southeastern United States could be attributed to the young stand age of pine plantations [*Sheffield and Dickson*, 1998] and the immature hardwood forests [*Brown et al.*, 1997]. Much of pine stands in the southern states were below maximum aboveground productivity [*Allen et al.*, 1990]. Intensive management of the southern pine forests could increase C uptake. Although this study was not designed for attribution of C sink to various mechanisms, the estimated carbon sink included all influences of those potential mechanisms that had been captured in remote sensing data for the estimated NPP increase trend [*Hicke et al.*, 2002]. However, mechanisms such as fire and land use change that influence carbon sinks by altering residence times and pool sizes to cause disequilibrium of C cycling processes were not fully accounted for in this analysis. Nevertheless, we did sensitivity analysis to evaluate uncertainties in parameter estimation under nonsteady state (Figures 9 and 10).

4.3. Uncertainties in Estimated Parameters and C Uptake

[49] This study estimated regional C uptake by quantifying a spatial pattern of C residence time together with a given NPP increase trend. We accordingly conducted extensive sensitivity analysis to evaluate various causes of uncertainties in estimated C residence times and C uptake. We ran the genetic algorithm 30 times to obtain standard errors of estimated 22 parameters for each of the eight biomes. Overall, most parameters were well constrained with relatively small standard errors except carbon partitioning coefficients (Figure 3). We have also used a probabilistic approach [*Xu et al.*, 2006] to evaluate uncertainties in inverted parameters for the regional analysis and found the majority of the parameters were well constrained (X. H. Zhou et al., Carbon residence time and sequestration in terrestrial ecosystems of the conterminous USA: A Bayes-

ian approach to uncertainty analysis, manuscript in preparation, 2008). In contrast, the number of parameters that can be constrained for ecosystem-scale analysis is very low. For example, the analysis of the covariance matrix in parameter estimation conducted by *Wang et al.* [2001] showed that only three or four parameters could be determined independently from the CO_2 flux observation. Multiple years of NEE data sets can constrain 13 parameters out of 23 in a Simplified Photosynthesis and Evapo-Transpiration model (SIPNET) by stochastic Bayesian inversion [*Braswell et al.*, 2005]. Six data sets of soil respiration, woody biomass, foliage biomass, litterfall, and soil carbon content from the Duke Forest Free-Air CO_2 Experiment (FACE) experiment can constrain four at ambient CO_2 and three at elevated CO_2 out of seven carbon transfer coefficients [*Xu et al.*, 2006]. The good constraint of parameter estimation by this regional analysis is due to the use of a very large set of various observations whereas those ecosystem-scale studies used a limited set of data in inverse analysis.

[50] Disequilibrium of carbon cycling processes under nonsteady state (Figure 7), caused by land use change (Figure 9) or influenced by different initial values of SOC (Figure 10) influenced estimated residence times and C uptake. So did variations in data (Figure 8). The analysis indicated that changes in observational data (Figure 8) or pool sizes (Figure 9) affected not only parameters that were directly related but also downstream parameters along C transfer processes. For example, a 20% increase in the leaf NPP resulted in increases in directly related parameters of maximum light-use efficiency (ε*) and allocation coefficient for leaves (α_L) but decreases in allocation coefficients for stems (α_W) and roots (α_R) because of the constraint of the sum of α_L, α_W, and α_R equaling 1. A decrease in α_R led to increases in C residence times for roots in three soil layers (τ_{R1}, τ_{R2}, and τ_{R3}). However, changes in SOC values hardly affect estimated values of any upstream parameters but strongly affected related parameters such as residence times and partitioning coefficients in the three soil carbon pools (Figures 8f, 8g, 8h, and 9). The model structure of C cycling processes is useful for analysis of uncertainties in parameter estimation with regard to observation errors in a particular data set.

[51] Disequilibrium caused by land use change and other disturbances is a major mechanism under C uptake (or release) as also showed by the sensitivity analysis in this study (Figure 10). Investigation and mapping of land use change and other disturbance are important to quantify carbon uptake, particularly in the human-impacted ecosystems. To quantify carbon sink caused by disequilibrium, we also need well-documented time series data of NPP, plant biomass, and SOC so that we can estimate residence times and initial values of pool sizes to assess nonsteady state carbon dynamics [*White et al.*, 2005] at regional scales.

5. Conclusions

[52] Terrestrial ecosystems play an important role in regulating atmospheric CO_2 concentration. Quantification of net ecosystem C uptake from the atmosphere at a regional scale requires identification of spatial patterns of both C residence times and NPP changes. In this study we used an inverse modeling method that combined a process-based model and genetic algorithm to estimate a spatial distribution of C residence times in the conterminous United States. The estimated residence times are highly heterogeneous over the conterminous United States, with most of the regions having values between 15 and 65 years. The averaged C residence time for the whole conterminous United States is 46 years. When the estimated residence times and the spatially heterogeneous NPP increases were incorporated into the forward modeling, the estimated total C uptake of the whole conterminous United States is 0.15 P g C a^{-1}, about one third of which were stored in soil. The cropland and grassland have a higher proportion of C uptaked in soil (47–70%) than do forests and woodlands (18–27%). Although the spatial pattern of net C uptake is controlled by both C residence times and rate of NPP change, we found that the proportion of soil C uptake is determined only by ecosystem C residence times and they are independent of the rate of NPP increase. Therefore the spatial patterns of C residence times are valuable for the evaluation of terrestrial ecosystem C sink.

Appendix A: Model Description

[53] In the TECO-R model, NPP is a function of the absorbed photosynthetically active radiation (APAR), maximum potential light-use efficiency (ε*), and temperature (T_ε) and moisture (W_ε) scalars that represent climate stresses on vegetation light-use efficiency. This relationship is expressed by

$$\mathrm{NPP} = f\mathrm{APAR} \cdot \mathrm{PAR} \cdot \varepsilon^* \cdot T_\varepsilon \cdot W_\varepsilon \tag{A1}$$

where fAPAR is a fraction of PAR that is absorbed by vegetation and determined by using a linear relationship between fAPAR and satellite-data derived normalized difference vegetation index (NDVI). Thus, APAR equals fAPAR times PAR. Solar radiation is converted to PAR by multiplying 0.5. In the TECO-R model, we used the same scalars as *Potter et al.* [1993] for T_ε and W_ε.

[54] The estimated NPP is allocated to plant tissues of leaves, stem, and roots according to the following equations:

$$\mathrm{NPP}_L = \alpha_L \mathrm{NPP} \tag{A2}$$

$$\mathrm{NPP}_W = \alpha_W \mathrm{NPP} \tag{A3}$$

$$\mathrm{NPP}_R = \alpha_R \mathrm{NPP} \tag{A4}$$

where α_L, α_W, α_R are allocation coefficients of NPP for leaves, wood, and roots, respectively. Thus, the C dynamics in leaf, stem, and root pools can be described by

$$\frac{dq_L}{dt} = \alpha_L \mathrm{NPP} - q_L/\tau_L \tag{A5}$$

$$\frac{dq_w}{dt} = \alpha_W \mathrm{NPP} - q_W/\tau_W \tag{A6}$$

$$\frac{dq_{R_j}}{dt} = \xi_{R_j}\alpha_R \mathrm{NPP} - q_{R_j}/\tau_{R_j},\ j = 1,2,3 \tag{A7}$$

where q_L, q_W, and q_{Rj} are C pool sizes in leaves, wood, and roots, respectively; τ_L, τ_W, and τ_{Rj} are carbon residence times in the pools of leaves, wood, and roots, respectively; the subscript R_j indicates three soil depths (0–20 cm, 20–50 cm, and 50–100 cm) for root biomass partitioning; and ξ_{Rj} are the partitioning coefficients of root biomass into three depths. The C dynamics in the litter and soil organic carbon (SOC) pools are partially determined by C transferred from plant biomass pools (Figure 1) and can be modeled by the first-order differential equations as

$$\frac{dq_F}{dt} = q_L/\tau_L + \eta q_C/\tau_c - q_F/\tau_F \tag{A8}$$

$$\frac{dq_C}{dt} = q_W/\tau_W - q_C/\tau_C \tag{A9}$$

$$\frac{dq_{S_1}}{dt} = q_{R_1}/\tau_{R_1} + \theta_F q_F/\tau_F + \theta_C q_C/\tau_C - q_{S_1}/\tau_{S_1} \tag{A10}$$

$$\frac{dq_{S_j}}{dt} = q_{R_j}/\tau_{R_j} + \theta_{S_{j-1}} q_{S_{j-1}}/\tau_{S_{j-1}} - q_{S_j}/\tau_{S_j}, j = 2,3 \tag{A11}$$

where q_F and q_C are C pool sizes for fine and coarse litter, respectively; q_{S1}, q_{S2}, and q_{S3} are pool sizes of SOC in three soil layers, respectively; τ_F, τ_C, τ_{S1}, τ_{S2}, and τ_{S3} are carbon residence times in fine litter, coarse litter, and SOC in three layers, respectively; η is a fraction of C exiting the coarse woody debris pool by mechanical break down; θ_F and θ_C are C partitioning coefficients of the fine litter and coarse litter pools, respectively; θ_{S1} and θ_{S2} are partitioning coefficients of soil C in the first and second soil layers, respectively.

[55] The carbon residence times in pools of litter and SOC (τ_F, τ_C, τ_{S1}, τ_{S2}, and τ_{S3}) vary with both climatic and biotic factors [*Schimel et al.*, 1994]. To specify the biotic influences on the residence times, the TECO-R model divided the conterminous United States into eight vegetation types on the basis of the 1-km land cover classification by *Hansen et al.* [2000] and then estimated the parameters separately. To quantify the impacts caused by spatial heterogeneity of climatic factors, the TECO-R model relates the site-specific residence times (τ_F, τ_C, τ_{S1}, τ_{S2}, and τ_{S3}) to the moisture and temperature corrected residence times (τ_F*,τ_C*, τ_{S1}*, τ_{S2}*, and τ_{S1}*) by

$$\tau_k = \tau_k^*/(W_s \cdot T_s), \qquad k = F, C, S_1, S_2, S_3 \tag{A12}$$

where W_s and T_s are moisture and temperature scalars for carbon residence times. The moisture scalar is estimated by monthly precipitation (*PPT*), potential evapotranspiration (*PET*), and soil moisture (*SoilM*) [*Randerson et al.*, 1996]:

$$\mathrm{SM} = \frac{\mathrm{PPT} + \mathrm{Soil}M}{\mathrm{PET}} \tag{A13a}$$

$$W_s = 0.1 + 0.9 \cdot \mathrm{SM} \qquad 0 \le \mathrm{SM} \le 1 \tag{A13b}$$

$$W_s = 1.0 \qquad 1 < \mathrm{SM} \le 2 \tag{A13c}$$

$$W_s = [1.0 + (1.0/28.0)] - (0.5/28.0)\mathrm{SM} \qquad 2 < \mathrm{SM} \le 30 \tag{A13d}$$

$$W_s = 0.5 \qquad 30 \le \mathrm{SM} \tag{A13e}$$

The temperature scalar of decomposition, T_s, is obtained directly from temperature data (T), as in the Century soil-carbon model [*Parton et al.*, 1987]:

$$T_s = \begin{cases} 1/(1 + 19e^{-0.16T}), & T < 45^\circ C \\ 10 - 0.2T, & 45 \le T \le 50^\circ C \\ 0, & T > 50^\circ C \end{cases} \tag{A14}$$

[56] **Acknowledgments.** We thank Jeffrey A. Hicke for sharing his research results on NPP change, and we thank Tao Xu for suggestions on the manuscript. We thank the data providers at NRCS, ORNL DAAC, GLCF, and Spatial Climate Analysis Service. This study was primarily supported by grants from the Terrestrial Carbon Program at the Office of Science, U.S. Department of Energy (DE-FG03-99ER62800), and from the National Science Foundation (DEB 0092642; DEB 0444518). The work was also partially supported by National Natural Science Foundation of China (40671173, 40401028, 30590384, and 40425008).

References

Allen, H. L., P. M. Dougherty, and R. G. Campbell (1990), Manipulation of water and nutrients: Practice and opportunity in southern United States pine forests, *For. Ecol. Manage.*, *30*(1–4), 437–453, doi:10.1016/0378-1127(90)90153-3.

Barrett, D. J. (2002), Steady state turnover time of carbon in the carbon in the Australian terrestrial biosphere, *Global Biogeochem. Cycles*, *16*(4), 1108, doi:10.1029/2002GB001860.

Bradford, J. B., W. K. Lauenroth, and I. C. Burke (2005), The impact of cropping on primary production in the U.S. great plains, *Ecology*, *86*(7), 1863–1872, doi:10.1890/04-0493.

Braswell, B. H., W. J. Sacks, E. Linder, and D. S. Schimel (2005), Estimating diurnal to annual ecosystem parameters by synthesis of a carbon flux model with eddy covariance net ecosystem exchange observations, *Global Change Biol.*, *11*, 335–355, doi:10.1111/j.1365-2486.2005.00897.x.

Brown, S., P. Schroeder, and R. Birdsey (1997), Aboveground biomass distribution of US eastern hardwood forests and the use of large trees as an indicator of forest development, *For. Ecol. Manage.*, *96*, 37–47, doi:10.1016/S0378-1127(97)00044-3.

Canadell, J. G., et al. (2007), Contributions to accelerating atmospheric CO_2 growth from economic activity, carbon intensity, and efficiency of natural sinks, *Proc. Natl. Acad. Sci. U.S.A*, doi:10.1073/pnas.0702737104.

Cannell, M. G. R. (1982), *World Forest Biomass and Primary Production Data*, 391 pp., Academic, London.

Cox, P. M., R. A. Betts, C. D. Jones, S. A. Spall, and I. J. Totterdell (2000), Acceleration of global warming due to carbon-cycle feedbacks in a coupled climate model, *Nature*, *408*, 184–187, doi:10.1038/35041539.

Cramer, W., et al. (2001), Global response of terrestrial ecosystem structure and function to CO_2 and climate change: Results from six dynamic global vegetation models, *Global Change Biol.*, *7*, 357–373, doi:10.1046/j.1365-2486.2001.00383.x.

Dai, A., and I. Y. Fung (1993), Can climate variability contribute to the "missing" CO_2 sink?, *Global Biogeochem. Cycles*, *7*(3), 599–609, doi:10.1029/93GB01165.

DeAngelis, D. L., R. H. Gardner, and H. H. Shugart (1997), NPP multibiome: Global IBP woodlands data, 1955–1975, data set, ORNL Distributed Active Archive Cent., Oak Ridge, Tenn. (Available at http://www.daac.ornl.gov).

de Vries, W., G. J. Reinds, P. Gundersen, and H. Sterba (2006), The impact of nitrogen deposition on carbon sequestration in European forests and forest soils, *Global Change Biol.*, *12*(7), 1151–1173, doi:10.1111/j.1365-2486.2006.01151.x.

Field, C. B., J. T. Randerson, and C. M. Malmstrom (1995), Global net primary production: Combining ecology and remote sensing, *Remote Sens. Environ.*, *51*, 74–88, doi:10.1016/0034-4257(94)00066-V.

Gaudinski, J. B., et al. (2001), The age of fine-root carbon in three forests of the eastern United States measured by radiocarbon, *Oecologia*, *129*, 420–429.

Goodale, C. L., et al. (2002), Forest carbon sinks in the Northern Hemisphere, *Ecol. Appl.*, *12*(3), 891–899, doi:10.1890/1051-0761(2002)012[0891:FCSITN]2.0.CO;2.

Hansen, M. C., R. S. Defries, J. R. G. Townshend, and R. Sohlberg (2000), Global land cover classification at 1 km spatial resolution using a classification tree approach, *Int. J. Remote Sens.*, *21*(6–7), 1331–1364, doi:10.1080/014311600210209.

Hicke, J. A., et al. (2002), Trends in North American net primary productivity derived from satellite observations, 1982–1998, *Global Biogeochem. Cycles*, *16*(2), 1018, doi:10.1029/2001GB001550.

Holland, E. A., et al. (1997), Variations in the predicted spatial distribution of atmospheric nitrogen deposition and their impact on carbon uptake by terrestrial ecosystems, *J. Geophys. Res.*, *102*(D13), 15,849–15,866, doi:10.1029/96JD03164.

Houghton, R. A. (2003), Why are estimates of the terrestrial carbon balance so different?, *Global Change Biol.*, *9*, 500–509, doi:10.1046/j.1365-2486.2003.00620.x.

Houghton, J. T., et al. (2001), *Climate Change 2001: The Scientific Basis*, 896 pp., Cambridge Univ. Press, New York.

Houghton, R. A., J. L. Hackler, and K. T. Lawrence (1999), The U.S. carbon budget: Contributions from land-use change, *Science*, *285*, 574–578, doi:10.1126/science.285.5427.574.

Lobell, D. B. (2002), Satellite estimates of productivity and light use efficiency in United States agriculture, 1982–98, *Global Change Biol.*, *8*, 722–735, doi:10.1046/j.1365-2486.2002.00503.x.

Luo, Y., L. Wu, A. Andrews, L. White, R. Matamala, K. V. R. Schafer, and W. H. Schlesinger (2001), Elevated CO_2 differentiates ecosystem carbon processes: Deconvolution analysis of Duke Forest FACE data, *Ecol. Monogr.*, *71*(3), 357–376.

Luo, Y., et al. (2003), Sustainability of terrestrial carbon sequestration: A case study in Duke Forest with inversion approach, *Global Biogeochem. Cycles*, *17*(1), 1021, doi:10.1029/2002GB001923.

Nemani, R. R., et al. (2003), Climate-driven increases in global terrestrial net primary production from 1982 to 1999, *Science*, *300*, 1560–1563, doi:10.1126/science.1082750.

Pacala, S. W., et al. (2001), Consistent land- and atmosphere-based U.S. carbon sink estimates, *Science*, *292*, 2316–2320, doi:10.1126/science.1057320.

Parton, W. J., D. S. Schimel, C. V. Cole, and D. S. Ojima (1987), Analysis of factors controlling soil organic matter levels in Great Plains grasslands, *Soil Sci. Soc. Am. J.*, *51*, 1173–1179.

Post, W. M., et al. (2004), Enhancement of carbon sequestration in US soils, *BioScience*, *54*(10), 895–908, doi:10.1641/0006-3568(2004)054[0895:EOCSIU]2.0.CO;2.

Potter, C. S., et al. (1993), Terrestrial ecosystem production: A process model based on global satellite and surface data, *Global Biogeochem. Cycles*, *7*(4), 811–841, doi:10.1029/93GB02725.

Randerson, J. T., M. V. Thompson, C. M. Malmstrom, C. B. Field, and I. Y. Fung (1996), Substrate limitations for heterotrophs: Implications for models that estimate the seasonal cycle of atmospheric CO_2, *Global Biogeochem. Cycles*, *10*(4), 585–602, doi:10.1029/96GB01981.

Raupach, M. R., et al. (2005), Model-data synthesis in terrestrial carbon observation: Methods, data requirements and data uncertainty specification, *Global Change Biol.*, *11*, 378–397, doi:10.1111/j.1365-2486.2005.00917.x.

Schimel, D. S., et al. (1994), Climatic, edaphic, and biotic controls over storage and turnover of carbon in soils, *Global Biogeochem. Cycles*, *8*(3), 279–293, doi:10.1029/94GB00993.

Schimel, D., et al. (2000), Contribution of increasing CO_2 and climate to carbon storage by ecosystems in the United States, *Science*, *287*, 2004–2006, doi:10.1126/science.287.5460.2004.

Schimel, D. S., et al. (2001), Recent patterns and mechanisms of carbon exchange by terrestrial ecosystems, *Nature*, *414*, 169–172, doi:10.1038/35102500.

Scurlock, J. M. O., K. R. Johnson, and R. J. Olson (2003), NPP Grassland: NPP estimates from biomass dynamics for 31 sites, 1948–1994, data set, ORNL Distributed Active Archive Cent., Oak Ridge, Tenn. (Available at http://www.daac.ornl.gov).

Sheffield, R. M., and J. G. Dickson (1998), The south's forestland: On the hot seat to provide more, in *Transactions of the 63rd North American Wildlife and Natural Resources Conference*, pp. 316–331, Wildlife Manage. Inst., Orlando, Fla.

Silver, W. L., and R. K. Miya (2001), Global patterns in root decomposition: Comparisons of climate and litter quality effects, *Oecologia*, *129*, 407–419.

Todd, D. E., and P. J. Hanson (2003), Rates of coarse-wood decomposition, in *North America Temperate Deciduous Forest Responses to Changing Precipitation Regimes,* edited by P. J. Hanson and S. D. Wullschleger, pp. 210–214, Springer, New York.

Turner, C. L. (1994), Plant biomass/production/consump[tion]. (FIFE), data set, ORNL Distributed Active Archive Cent., Oak Ridge, Tenn. (Available at http://www.daac.ornl.gov)

Vogt, K. A., et al. (1996), Review of root dynamics in forest ecosystems grouped by climate, climatic forest type and species, *Plant Soil*, *187*, 159–219, doi:10.1007/BF00017088.

Wang, Y. P., R. Leuning, H. A. Cleugh, and P. A. Coppin (2001), Parameter estimation in surface exchange models using nonlinear inversion: How many parameters can we estimate and which measurements are most useful?, *Global Change Biol.*, *7*, 495–510, doi:10.1046/j.1365-2486.2001.00434.x.

White, L. W., Y. Luo, and T. Xu (2005), Carbon sequestration: Inversion of FACE data and prediction, *Appl. Math. Comput.*, *163*, 783–800, doi:10.1016/j.amc.2004.04.021.

Xu, T., L. White, D. Hui, and Y. Luo (2006), Probabilistic inversion of a terrestrial ecosystem model: Analysis of uncertainty in parameter estimation and model prediction, *Global Biogeochem. Cycles*, *20*, GB2007, doi:10.1029/2005GB002468.

Zhang, D., D. Hui, Y. Luo, and G. Zhou (2008), Rates of litter decomposition in terrestrial ecosystems: Global patterns and controlling factors, *J. Plant Ecol.*, *1*(2), 85–93, doi:10.1093/jpe/rtn002.

Y. Luo, Department of Botany and Microbiology, University of Oklahoma, Norman, OK 73019, USA. (yluo@ou.edu)

T. Zhou, State Key Laboratory of Earth Surface Processes and Resource Ecology, Beijing Normal University, 19 Xinjiekouwai Street, Beijing 100875, China. (tzhou@bnu.edu.cn)